# Non-Markovianity of colored noisy channels

Claudia Benedetti,[1] Matteo G. A. Paris,[1] and Sabrina Maniscalco[2]
[1]*Dipartimento di Fisica, Università degli Studi di Milano, I-20133 Milano, Italy*
[2]*Scottish Center for Quantum Physics Alliance, Engineering and Physical Sciences, Department of Physics, Heriot-Watt University, Edinburgh EH14 4AS, Scotland, United Kingdom*
(Received 2 October 2013; published 16 January 2014)

We address the non-Markovian character of quantum maps describing the interaction of a qubit with a random classical field. In particular, we evaluate trace- and capacity-based non-Markovianity measures for two relevant classes of environments showing non-Gaussian fluctuations, described respectively by random telegraph noise and colored noise with spectra of the the form $1/f^{\alpha}$. We analyze the dynamics of both the trace distance and the quantum capacity, and show that the behavior of non-Markovianity based on both measures is qualitatively similar. Our results show that environments with a spectrum that contains a relevant low-frequency contribution are generally non-Markovian. We also find that the non-Markovianity of colored environments decreases when the number of fluctuators realizing the environment increases.

DOI: 10.1103/PhysRevA.89.012114 PACS number(s): 03.65.Yz, 03.65.Ta

## I. INTRODUCTION

The unavoidable interaction of a quantum system with its environment usually destroys its coherence and quantumness [1,2]. The fragile quantum information encoded in an open quantum system is lost due to the presence of the environment that continuously monitors the system. Nevertheless, in some cases the lost information can be partly restored due to non-negligible correlations between system and environment. We refer to the systems in which such recoherence phenomena occur as non-Markovian open quantum systems. The dynamics of open quantum systems has been often described using the Born-Markov approximation leading to a master equation of the Lindblad form [3]. This approximation, however, neglecting system-bath-induced memory effects, does not lead to a correct description of the dynamics of many relevant systems in quantum optics and solid-state physics, and cannot be used in certain quantum information processing scenarios [4–9]. In addition, in the spirit of reservoir engineering, one can induce non-Markovianity to improve quantum protocols such as quantum metrology and quantum key distribution [10–14].

The concept of non-Markovianity is not uniquely defined in the literature. Several measures have been proposed in recent years [14–20] and, in general, these measures do not coincide in detecting non-Markovianity. In this paper we focus on two measures of non-Markovianity: the Breuer-Laine-Piilo (BLP) measure [16] based on state distinguishability, and the Bylicka-Chruściński-Maniscalco (BCM) measure [14] based on entanglement-assisted and/or quantum capacities. In the first case the characteristic trait of non-Markovianity is a back flow of information, i.e., a partial increase in state distinguishability, while in the second case memory effects are identified with a regrowth of channel capacities.

It is known that for single qubit dephasing channels, as those considered in the following, the Markovian or non-Markovian character of the dynamical map coincides for all measures. Therefore, it is sufficient to study one of them. In this paper we focus on both the BLP measure and the BCM measure as we are interested not only in understanding information back flow but also in investigating under which conditions qubit channels subject to random classical noise may be exploited for reliably transmitting quantum and classical information. Moreover, the BCM measure provides us with a rigorous information theoretical description of memory effects by linking the amount of information on the system to the amount of information on the environment, and therefore allowing us to properly define the concept of information flow.

We focus on non-Markovianity arising in classical environments exhibiting non-Gaussian fluctuations, i.e., described by random non-Gaussian fields. In particular, we address the influence of this class of environments on the dynamics of a qubit. As a matter of fact, little attention has been paid to non-Markovianity in classical environments; most of the existing studies are devoted to time-independent random fields or to Gaussian dynamic noise [21–24]. On the other hand, stochastic processes characterized by non-Gaussian fluctuations are very common in nature and have received large attention [25–28]. A stochastic process is non-Gaussian if it cannot be fully characterized by the mean and variance. As a consequence, the mere knowledge of the spectrum is not sufficient to describe the process, and the very structure of environment plays a role in determining its influence on the coherence properties of quantum systems [29].

In this paper we focus on two relevant classes of non-Gaussian noise: the random telegraph noise (RTN) with a Lorentzian spectrum and the family of low-frequency noise with $1/f^{\alpha}$ spectrum. The RTN is generated from a bistable fluctuator flipping between two values with a switching rate $\xi$. RTN allows one to model environmental noise appearing in many semiconducting and superconducting nanodevices [30–35]. Noises with $1/f^{\alpha}$ spectra are found when the environment can be described as a collection of $N_f$ random bistable fluctuators, with $N_f \geqslant 1$. It affects solid-state devices, superconducting qubits, and magnetic systems [36–41]. The dynamical map of a qubit interacting with these kind of environments describes pure dephasing. In this case the channel is degradable and the entanglement-assisted capacity coincides with the quantum channel capacity, hence we will consider only the latter one in the rest of the paper. Moreover, a simple analytical expression for the dynamics of both the trace distance and the quantum capacity exists,

 

allowing us to analyze in detail the non-Markovian dynamics as a function of the noise parameters. Our results show that the two measures display a qualitatively similar behavior, leading to a consistent assessment of non-Markovianity. We also find that environments with a spectrum dominated by low-frequency contribution are generally non-Markovian and that the non-Markovianity of colored environments is progressively destroyed when the number of fluctuators realizing the environment increases. These results confirm that non-Markovianity may represent a resource for quantum information processing. Indeed, we found that, in dephasing channels, back flow of information corresponds to revivals of quantum correlations [29]. Finally, upon assuming that the channel is reset after each use, we discuss how reliable transmission of information through a noisy quantum channel may be achieved, even in presence of classical non-Gaussian noise, for properly engineered structured environments.

In principle, one could quantify non-Markovianity of classical random fields using the definition of non-Markovianity for classical stochastic processes, i.e., in terms of the Kolmogorov hierarchy of the $n$-point joint probability distributions. In turn, it has been proved [42,43] that there are clear differences between the classical and the quantum notion of non-Markovianity. In this paper, since we are interested in the *effects* of non-Markovianity on the quantum information carrier rather than in addressing the fundamental properties of the environment, we have explicitly chosen to assess non-Markovianity of classical noise in terms of quantum measures of non-Markovianity for the quantum channels induced on qubit systems. This approach allows us to assess classical environments in terms of their effects on quantum systems and, possibly, engineer their structure.

This paper is organized as follows. In Sec. II we introduce the BLP and BCM measures of non-Markovianity. In Sec. III we describe in some details the physical model employed throughout the paper. In Sec. IV we show our results on the dynamics of the non-Markovianity measures. Section V closes the paper with concluding remarks.

## II. NON-MARKOVIANITY MEASURES

In this section we review two measures of non-Markovianity: the BLP measure [16], based on the trace distance, and the BCM measure, based on the quantum capacity [14].

### A. BLP measure

The underlying idea behind the BLP measure is that Markovian processes tend to reduce the distinguishability between any two states of the open system, while non-Markovian processes are characterized by a partial regrowth of distinguishability on at least a subset of states. The loss of distinguishability is interpreted as an irreversible loss of information on the system while restored distinguishability reflects a partial, and often temporary, increase of information about the system. Since the trace distance is related to the probability of successfully distinguishing two quantum states $\rho_1$ and $\rho_2$, it seems natural to use this quantity to describe memory effects and non-Markovianity. The trace distance is defined as:

$$D(\rho_1,\rho_2) = \tfrac{1}{2}\mathrm{Tr}|\rho_1 - \rho_2|, \tag{1}$$

where $|A| = \sqrt{A^\dagger A}$. The trace distance defines a metric on the space of density matrices and $0 < D < 1$. Any completely positive and trace-preserving map $\Phi(t)$ is a contraction for this metric:

$$D(\Phi(t)\rho_1,\Phi(t)\rho_2) < D(\rho_1,\rho_2). \tag{2}$$

The flux of information is then defined as:

$$\sigma(t,\rho_{1,2}(0)) = \frac{d}{dt}D(\rho_1,\rho_2), \tag{3}$$

where $\rho_{1,2}(0)$ denotes the density matrix of the initial states. A loss in distinguishability is linked to a negative information flux $\sigma(t,\rho_{1,2}(0)) < 0$, while positive flux describes an increasing distinguishability between two quantum states. The BLP measure of non-Markovianity quantifies the total amount of information back flow into the system:

$$N_{\mathrm{BLP}} = \max_{\rho_{1,2}(0)} \int_{\sigma>0} ds\, \sigma(s,\rho_{1,2}(0)), \tag{4}$$

where the maximization is over all pairs of initial states and the integration is over all time intervals where the flux is positive. Whenever $N_{\mathrm{BLP}} > 0$ the dynamics is non-Markovian. It is possible to show that all divisible maps are Markovian according to this measure, but the converse is not true in general [44]. Generally, calculating $N_{\mathrm{BLP}}$ is a difficult task, because of the maximization procedure involved. Nevertheless, maximizing pairs have been found for certain classes of noisy channels, such as the dephasing channel we are going to deal with. As we will review in Sec. III, indeed, the dephasing dynamics of the qubit is described by the following map

$$\rho(t) = \frac{1+\Gamma(t)}{2}\rho(0) + \frac{1-\Gamma(t)}{2}\sigma_z\rho(0),\sigma_z, \tag{5}$$

i.e., $\rho_{ij}(t) = \rho_{ij}(0)\Gamma(t)$, with $\Gamma(t)$ the dephasing function. Notice that in Eq. (5) dephasing is induced by a classical stochastic process. It follows that the coefficient $\Gamma(t)$ is a real quantity that can assume positive and negative values between $\pm 1$. For the sake of clarity we notice here the difference between this model and the spin-boson model describing pure dephasing arising from the interaction with a quantum environment [45,46]. In the latter case the dynamics of the coherences is given by $\rho_{ij}(t) = \rho_{ij}(0)\exp[-f(t)]$, with $f(t) \geqslant 0$, and therefore the dephasing function is always positive.

For a qubit interacting with a classical random field, as in Eq. (5), the optimal pair in Eq. (4) that maximizes the increase of the trace distance has been found [47]. In the following, we use the name *optimal trace distance* for the expression of the trace distance in Eq. (1) computed for the optimal pair. Thus, the study of BLP non-Markovianity can be reduced to the analysis of the optimal trace distance. In our case this quantity reads:

$$D(t) = |\Gamma(t)|, \tag{6}$$

which is the absolute value of the dephasing function $\Gamma(t)$. Once the expression of $D(t)$ is known it is possible to write the information flux (3) and then numerically compute the

non-Markovianity as the integral of the information flux over the time intervals in which it is positive.

### B. BCM measure

The second measure that we will use, introduced by Bylicka, Chruściński, and Maniscalco, is based on the channel capacities [14]. As mentioned above, we focus here on the quantum channel capacity as, in our case, it coincides with the entanglement-assisted capacity. Generally, the quantum capacity bounds the rate at which quantum information can be reliably transmitted through a noisy quantum channel $\Phi(t)$. Dephasing is a degradable channel and thus the single-use quantum capacity may be written as

$$C_Q(\Phi(t)) = \sup_{\rho} I_c(\rho, \Phi(t)) \tag{7}$$

where $I_c$ represents the coherent information:

$$I_c(\rho, \Phi(t)) = S(\Phi(t)\rho) - S(\rho, \Phi(t)), \tag{8}$$

where $S(\rho) = -\mathrm{Tr}[\rho \ln \rho]$ is the Von-Neumann entropy of the state $\rho$ and $S(\rho, \Phi(t))$ the entropy exchange [48]. The superior should be taken over all the possible states of the information carrier. The latter quantity measures the change in the entropy of the environment. It is worth stressing that, contrarily to trace distance, the coherent information describes how the entropy of both the system and the environment change. Hence this quantity is more apt to capture the concept of information flow between system and environment. More explicitly, coherent information is, in fact, quantifying the flow of information between the system and the environment, while the trace distance is quantifying only the *loss* of information that we have *on the system* without any indication on whether this information is acquired by another agent (and may come back). The fact that the two measures agree confirms, at least for dephasing channels, that the trace distance may be considered a measure of the flow of information from the system to the environment.

Strictly speaking, Eq. (7) describes the quantum capacity only for memoryless degradable channels [49–51] and thus it seems unsuitable to address quantum channels arising from the interaction with a classical environment exhibiting long-lasting time correlations. However, we are interested in the effects of memory *during the propagation* of the information carriers, rather than memory effects among subsequent uses of the channel, and thus the expression in (7) fits nicely for our purposes. Of course, memory effects among uses should be eventually addressed in view of realistic implementations. Our results should be considered as a first step toward a complete analysis of this class of channels, including both types of memory effects [52].

As a consequence of the quantum data-processing inequality, the quantum capacity of divisible channels is a monotonically decreasing function of time. The BCM measure is therefore based on the nonmonotonic behavior of $C_Q(\Phi(t))$:

$$N_{\mathrm{BCM}} = \int_{\frac{dC_Q(\Phi(t))}{dt} > 0} \frac{d\, C_Q(\Phi(t))}{dt}\, dt. \tag{9}$$

Non-Markovianity corresponds to $N_{\mathrm{BCM}} > 0$. Even if this measure does not explicitly involve a maximization procedure, an optimization is required in the computation of the quantum capacity (7). In the case of a dephasing channel, however, the analytical expression for $C_Q(\Phi(t))$ is known [53]:

$$C_Q(t) = 1 - H_2\left(\frac{1-\Gamma(t)}{2}\right), \tag{10}$$

with $H_2(p) = -p \ln p - (1-p)\ln(1-p)$ the Shannon binary entropy. As we will see in the following, the operational interpretation of the quantum capacity allows us to use $N_{\mathrm{BCM}}$ to assess if and how non-Markovianity can be seen as a resource for quantum communication and information processing.

Both the BLP and the BCM measure consistently detect non-Markovianity in the case of a dephasing channel. It is easy to show that in both cases the dynamics is non-Markovian in the following two regimes:

$$\begin{aligned} &\frac{d\Gamma(t)}{dt} < 0 \quad \text{and} \quad \Gamma(t) < 0, \\ &\frac{d\Gamma(t)}{dt} > 0 \quad \text{and} \quad \Gamma(t) > 0, \end{aligned} \tag{11}$$

where $\Gamma(t)$ is the real coefficient appearing in Eq. (5)

## III. PHYSICAL MODEL

In order to characterize the non-Markovian features of a noisy channel one has to probe its influence on an information carrier. Here we focus attention on the simplest quantum probe, i.e., a qubit, and infer the properties of the channel by analyzing the decoherence process induced on the qubit. We model the classical environment as a random field described by a stochastic process $c(t)$. In order to model the colored noisy channel we do not make the usual assumption of a Gaussian process, while we only assume the stationarity property.

Let us consider a generic qubit described by the state vector

$$|\psi_0\rangle = \alpha|0\rangle + \beta|1\rangle, \tag{12}$$

satisfying the condition $|\alpha|^2 + |\beta|^2 = 1$. We assume that the evolution of the qubit is governed by the Hamiltonian

$$H(t) = \epsilon\, \sigma_z + \nu\, c(t)\sigma_z, \tag{13}$$

where $\epsilon$ is the energy splitting between the two levels of the qubit, $\nu$ is a coupling constant, and $\sigma_z$ is the Pauli matrix. The system-environment interaction of Eq. (13) describes a nondissipative dephasing channel, and it is suitable to portray situations where the typical frequencies of the environment are smaller than the natural frequency of the qubit.

Different expressions for $c(t)$ may be employed, corresponding to different kinds of classical noise. In the next sections, we briefly review the dynamics of the generic qubit state (12) in environments characterized by RTN and colored noise spectra of the form $\frac{1}{f^\alpha}$. Then, in Sec. IV we will employ these results to explicitly evaluate the non-Markovianity of the corresponding channels.

### A. Random telegraph noise

Random telegraph noise is very common in nature. It appears in semiconductor, metal, and superconducting

devices [30–35]. The source of random telegraph noise is a bistable fluctuator, which is a quantity which flips between two values with a switching rate, such as a resistance switching between two discrete values, charges jumping between two different locations, or electrons that flip their spin. In order to describe a RTN, the quantity $c(t)$ in Eq. (13) flips randomly between values $\pm 1$ with a switching rate $\xi$. This noise is characterized by an exponential decaying autocorrelation function $C(t,t_0)$ and a Lorentzian spectrum $S(\omega)$:

$$C(t,t_0) = e^{-2\xi\,|t-t_0|}, \tag{14}$$

$$S(\omega) \propto \frac{4\xi}{4\xi^2+\omega^2}. \tag{15}$$

Hereafter we use dimensionless quantities. In particular we introduce the dimensionless time $\tau \equiv \nu t$ and switching rate $\gamma \equiv \xi/\nu$. The dynamics of the global system is described in the interaction picture by the evolution operator $U(\tau) = e^{-i\varphi(\tau)\sigma_z}$ where

$$\varphi(\tau) = \int_0^\tau c(s)ds$$

is the RTN phase [54]. The qubit density matrix is obtained as the average of the evolved density operator over the process, i.e., over the RTN phase:

$$\rho(\tau,\gamma) = \langle U(\tau)\rho_0 U^\dagger(\tau)\rangle_{\varphi(\tau)} \tag{16}$$

where $\rho_0 = |\psi_0\rangle\langle\psi_0|$. The qubit density matrix thus has the expression:

$$\rho(\tau,\gamma) = \begin{pmatrix} |\alpha|^2 & \alpha\beta^*\, G(\tau,\gamma) \\ \alpha^*\beta\, G(\tau,\gamma) & |\beta|^2 \end{pmatrix}, \tag{17}$$

where the $z^*$ denotes the conjugate of the complex number $z$. The coefficient $G(\tau,\gamma) = \langle e^{2i\varphi(\tau)}\rangle$ corresponds to the function $\Gamma(t)$ in Eq. (5), and is given by:

$$G(\tau,\gamma) = e^{-\gamma\tau}\left(\cosh\delta\tau + \frac{\gamma\sinh\delta\tau}{\delta}\right), \tag{18}$$

with $\delta = \sqrt{\gamma^2-4}$.

### B. Colored noise

Power-law frequency noise characterized by $1/f^\alpha$ spectrum is a ubiquitous noise in nature [36]. It can be found in nanoscale electronic devices where it manifests as charge fluctuations [37,38] and in Josephson circuits due to fluctuating background charges and flux [39–41]. Typical values of the coefficient $\alpha$ range between 0.5 and 2. $1/f^\alpha$ noise arises when the environment is described as a collection of bistable fluctuators [29]. Every fluctuator has an unknown switching rate, taken from the ensemble $\{\gamma_i, p_\alpha(\gamma_i)\}$, where the probability distribution is:

$$p_\alpha(\gamma) = \begin{cases} \frac{1}{\gamma\,\ln(\gamma_2/\gamma_1)} & \alpha = 1 \\ \frac{\alpha-1}{\gamma^\alpha}\left[\frac{(\gamma_1\gamma_2)^{\alpha-1}}{\gamma_2^{\alpha-1}-\gamma_1^{\alpha-1}}\right] & \alpha \neq 1. \end{cases} \tag{19}$$

The coefficient $c(t)$ in Hamiltonian (13) is a linear superposition of $N_f$ random bistable fluctuators, $c(t) = \sum_i^{N_f} c_i(t)$, where every $c_i(t)$ describes a stochastic telegraphic process with a Lorentzian spectrum. Following Ref. [29], we can write the global noise phase as the product of RTN phases, $\varphi(\tau) = \prod_i^{N_f}\varphi_i(\tau)$. The evolution operator in the interaction picture is written as $U(\tau) = e^{-i\varphi(\tau)\sigma_z}$. The qubit density matrix is obtained as an average of the global density matrix $U(\tau)\rho_0 U^\dagger(\tau)$ over the total noise phase and the switching rates:

$$\rho(\tau) = \int_{\gamma_1}^{\gamma_2} \rho(\tau,\gamma)\; p_\alpha(\gamma)\; d\gamma, \tag{20}$$

where now $\rho(\tau,\gamma)$ has the same expression as in Eq. (16) but the average is over the global phase, $\gamma_1$ and $\gamma_2$ are the smallest and the biggest switching rate considered. The qubit density matrix can thus be written as:

$$\rho(\tau) = \begin{pmatrix} |\alpha|^2 & \alpha\beta^*\;\Lambda(\tau,\alpha,N_f) \\ \alpha^*\beta\;\Lambda(\tau,\alpha,N_f) & |\beta|^2 \end{pmatrix}. \tag{21}$$

where

$$\Lambda(\tau,\alpha,N_f) = \left[\int_{\gamma_1}^{\gamma^2} G(\tau,\gamma)\; p_\alpha(\gamma)\; d\gamma\right]^{N_f}. \tag{22}$$

Also in this case the dephasing factor $\Lambda(\tau,\alpha,N_f)$ in Eq. (21) corresponds to the coefficient $\Gamma(t)$ in Eq. (5).

## IV. NON-MARKOVIANITY OF NON-GAUSSIAN NOISY CHANNELS

The trace distance as well as the quantum capacity depends only on the dephasing factor in the density matrices in Eqs. (17) and (21). Thus their behavior, even if quantitatively different, is qualitatively the same. It immediately follows that also $N_{\mathrm{BLP}}$ and $N_{\mathrm{BCM}}$ depend only on the dephasing factor and are characterized by the same behavior. For any given values of the interaction time, $N_{\mathrm{BLP}}$ and $N_{\mathrm{BCM}}$ are functions of noise parameters describing the channels. In the case of RTN, there is a single parameter, i.e., the switching rate $\gamma$, whereas for colored noise with $1/f^\alpha$ spectra the tunable parameters are the exponent $\alpha$ and the number of fluctuators.

In this section we study the non-Markovian character of qubits subjected to RTN and colored noise. In the spirit of reservoir engineering this allows one to single out the values of noise parameters minimizing dephasing and/or leading to to environment-induced recoherence, i.e., non-Markovianity. Similarly, we will see how the study of the behavior of the quantum capacity as a function of time reveals the existence of specific channel lengths (interaction times) permitting a reliable transmission of information even in presence of high levels of noise. Finally, we will conclude our analysis with the characterization of non-Markovianity of classical environments acting on two-qubit states and show that the non-Markovianity is quantitatively the same as the single-qubit case for both measures.

### A. Random telegraph noise

The first step to compute the BLP and BCM non-Markovianity measures is the evaluation of the optimal trace distance and the quantum capacity, respectively. From Eqs. (6)

and (10), we can write:

$$D(\tau,\gamma) = |G(\tau,\gamma)|, \tag{23}$$

$$C_Q(\tau,\gamma) = 1 - H_2\left(\frac{1-G(\tau,\gamma)}{2}\right), \tag{24}$$

with $G(\tau,\gamma)$ given by Eq. (18). Two different regimes naturally arise: for $\gamma < 2$ both the trace distance and the quantum capacity display damped oscillations, i.e., the dynamics is non-Markovian, whereas for $\gamma \geqslant 2$ they decay monotonically, i.e., the dynamics is Markovian. In fact, the non-Markovianity measures $N_{\rm BLP}$ and $N_{\rm BCM}$ correspond to the integrals, over their range of positivity, of the quantities

$$\begin{aligned}\sigma_{\rm BLP} &= \frac{d}{d\tau}D(\tau,\gamma) = -\gamma\,|G(\tau,\gamma)| \\ &\quad + \mathrm{sgn}\,[G(\tau,\gamma)]\,(\gamma\cosh\delta\tau + \delta\sinh\delta\tau)\,e^{-\gamma\tau} \\ &= -4\,e^{-\gamma\tau}\,\frac{\sinh\delta\tau}{\delta} \qquad \text{if } \gamma \geqslant 2 \\ \sigma_{\rm BCM} &= \frac{d}{d\tau}C_Q(\tau,\gamma) = -\frac{4}{\ln 2}\,\frac{\sinh\delta\tau}{\delta}\,\mathrm{arctanh}\,G(\tau,\gamma)\end{aligned} \tag{25}$$

respectively, where $G(\tau,\gamma)$ is given in Eq.(18). As it is apparent from their expressions, and from the fact that $G(\tau,\gamma) \geqslant 0$ for $\gamma \geqslant 2$, both the $\sigma$'s are negative definite for $\gamma \geqslant 2$, such that both the measures $N_{\rm BLP}$ and $N_{\rm BCM}$ vanish for $\gamma \geqslant 2$. On the other hand, both the $\sigma$'s show an oscillatory behavior as a function of time, which includes positive values, for any values of $\gamma < 2$.

Using Eq. (25) one finds the extrema of the functions $D(\tau,\gamma)$ and $C_Q(\gamma,\tau)$ and thus the regions where they are increasing function of time. Maxima are located at $\tau_k = k\pi/\sqrt{4-\gamma^2}$ and minima (where the two functions vanish) at $\tau_k - \tau^*$, with $\tau^* = (4-\gamma^2)^{-\frac{1}{2}}\mathrm{arctanh}[\gamma(4-\gamma^2)^{\frac{1}{2}}]$. We thus obtain

$$N_{\rm BLP} = \sum_{k=1}^{\infty} D(\gamma,\tau_k) = \left[\exp\left(\frac{\pi\gamma}{\sqrt{4-\gamma^2}}\right) - 1\right]^{-1} \tag{26}$$

$$N_{\rm BCM} = \sum_{k=1}^{\infty} C_Q(\gamma,\tau_k). \tag{27}$$

In the upper panel of Fig. 1 we show the trace distance dynamics in the non-Markovian regime $\gamma < 2$ for three specific values of $\gamma$. We notice that the smaller is $\gamma$, the higher are the revivals of the trace distance, and thus the more enhanced is the non-Markovian character of the dynamics. A similar behavior occurs for the quantum capacity. Indeed, one can see from the lower panel of Fig. 1 that both $N_{\rm BLP}$ and $N_{\rm BCM}$ increase for decreasing values of $\gamma$. From a physical point of view this reflects the fact that small values of $\gamma$ correspond to non-negligible and long-living environmental correlations, as described by the autocorrelation function of Eq. (14), and therefore to more pronounced memory effects. The lower panel of Fig. 1 also shows that $N_{\rm BCM}$ decays faster than $N_{\rm BLP}$ as a function of $\gamma$. On the other hand, as mentioned above, the threshold between the Markovian and non-Markovian regime is the same for both measures and corresponds to $\gamma = 2$, for which both measures vanish. More precisely, for $\gamma \geqslant 2$ both the measures are identically zero since the time derivatives of both the trace distance and the quantum capacity are negative definite, meaning that information permanently leaks away from the system.

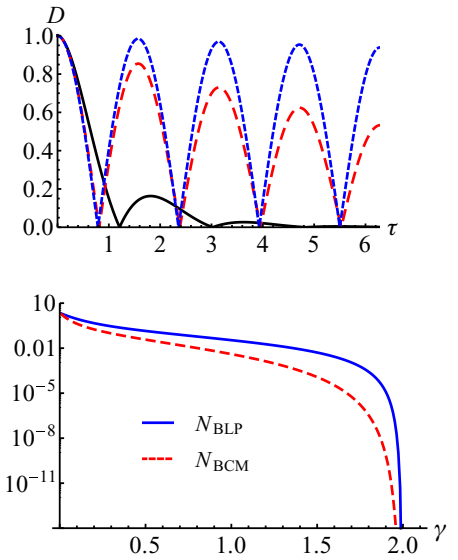


FIG. 1. (Color online) Non-Markovianity of RTN channels. The upper panel shows the trace distance as a function of time for three different values of the switching rate: $\gamma = 1$ (solid black line), $\gamma = 0.1$ (dashed red line), and $\gamma = 0.01$ (dotted blue line). The lower panel is a log plot of both BLP and BCM non-Markovianity measures as a function of $\gamma$.

### B. Colored $1/f^\alpha$ noise

For the sake of conciseness we focus initially on the behavior of trace distance, as the dynamics of the quantum capacity is qualitatively similar. For colored noise with spectrum $1/f^\alpha$, the optimal trace distance is:

$$D(\tau,\alpha,N_f) = |\Lambda(\tau,\alpha,N_f)|. \tag{28}$$

This quantity cannot be evaluated analytically since the integral in Eq. (22) is not analytically solvable. We computed it numerically upon assuming that the range of integration in Eq. (22) includes rates belonging to the interval $[\gamma_1,\gamma_2] = [10^{-4},10^4]$.

The optimal trace distance for a generic number of fluctuators may be written in terms of the same quantity for a single fluctuator as follows

$$D(\tau,\alpha,N_f) = D(\tau,\alpha,1)^{N_f}. \tag{29}$$

We thus first analyze the non-Markovianity of a colored environment generated by a single random fluctuator. For a fixed value of $\alpha$ and $N_f = 1$ the trace distance is always a nonmonotonic function of time, as illustrated in Fig. 2. Therefore, contrarily to the case of RTN, the dynamics is always non-Markovian for a single fluctuator. However, one can still identify two regimes depending on the value of $\alpha$.

For, $\alpha \geqslant 1$ the optimal trace distance is characterized by pronounced oscillations in time between zero and a maximum

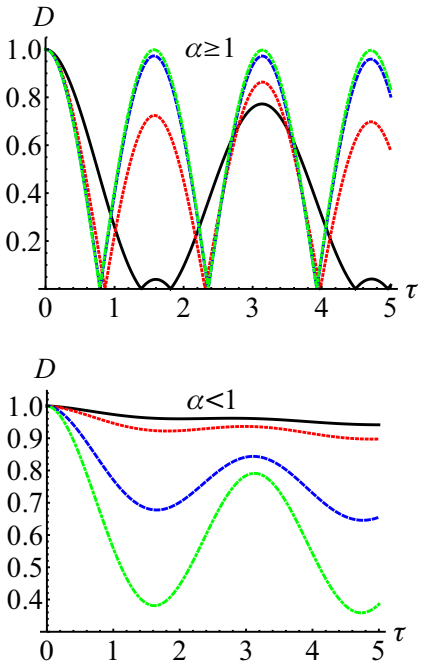


FIG. 2. (Color online) Non-Markovianity of colored channels. The upper panel shows the trace distance for a qubit subject to $1/f^{\alpha}$ noise generated by a single random fluctuator for different values of $\alpha \geqslant 1$: $\alpha = 1$ (solid black line), $\alpha = 1.3$ (dotted red line), $\alpha = 1.5$ (dashed blue line), and $\alpha = 2$ (dot-dashed green line). The lower panel shows the same quantity for values of $\alpha < 1$: $\alpha = 0.5$ (solid black line), $\alpha = 0.6$ (dotted red line), $\alpha = 0.8$ (dashed blue line), and $\alpha = 0.9$ (dot-dashed green line).

value, which depends upon the value of $\alpha$. The larger is $\alpha$, the larger are the local maxima. For $\alpha = 1$ higher and lower maxima alternate periodically at times $\tau = \pi/2$. As $\alpha$ increases, the height of the alternating peaks increases until it becomes uniform, as shown in Fig. 2(a). For $\alpha < 1$, $D$ is still nonmonotonic, but the oscillations are less noticeable and the optimal trace distance never vanishes. This case is illustrated in Fig. 2(b). Generally, as $\alpha$ decreases, the amplitude of the oscillations in the trace distance decreases, both in the $\alpha < 1$ and in the $\alpha \geqslant 1$ region of parameter space. Non-Markovianity is thus stronger for systems interacting with environments with a dominant low-frequency component in the frequency spectrum. By changing the range of integration in Eq. (22), we can analyze the contribution of small and large switching rates on non-Markovianity. In particular, in Fig. 3 we compare the behavior of the trace distance for two mutually exclusive ranges of integration, namely for $\gamma \in [10^{-4},2]$ and $\gamma \in [2,10^{4}]$. In the first case we integrate only over small values of the switching rates, and the trace distance exhibits revivals, revealing the presence of information back flow. In the second case the integration is performed over big values of $\gamma$ and, as a result, $D(t,\alpha,1)$ decays monotonically. This behavior is consistent with the results obtained for the RTN channel: memory effects are dominant for low switching rates, i.e., longer correlation times. Thus non-Markovianity is a distinctive trait of low-frequency noise spectrum.

We now consider the more realistic case of a larger number of fluctuators. From Eq. (29), and remembering that

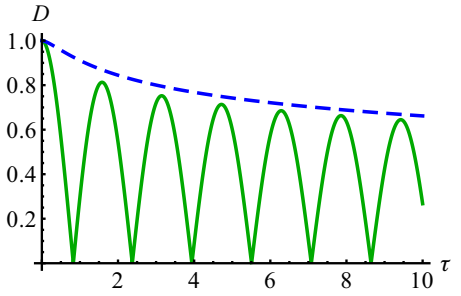


FIG. 3. (Color online) Non-Markovianity of colored channels. The plot shows the trace distance as a function of time for $\alpha = 1$. The two curves refer two different ranges of integration in Eq. (22): $[10^{-4},2]$ (green solid line) and $[2,10^{4}]$(blue dashed line).

$0 \leqslant D \leqslant 1$, one sees immediately that the overall effect of having a large number of fluctuators is to decrease the value of the optimal trace distance. As a consequence, oscillations in the trace distance are damped and may disappear, depending also on the value of $\alpha$, leading to a monotonic decay. This behavior is illustrated in Fig. 4, where $N_{\mathrm{BLP}}$ and $N_{\mathrm{BCM}}$ are plotted as a function of the numbers of fluctuators and for three different exemplary values of $\alpha$. The figure clearly shows that for smaller values of $\alpha$, i.e., in the $\alpha < 1$ regime, a small number of fluctuators is sufficient to completely wash out memory effects. For increasingly larger values of $\alpha$, non-Markovianity persists also for $N_f \approx 100$. Generally, increasing the number of fluctuators brings the system towards a Markovian dynamics. Summarizing, non-Markovianity is typical of environments with a small number of fluctuators and a noise spectrum dominated by low frequencies.

Let us now analyze the behavior of the quantum channel capacity. In Fig. 5 we consider as an example the case of ten random fluctuators and different values of $\alpha$. As expected, $C_Q(\tau,\alpha,N_f)$ is an increasing function of $\alpha$. It has revivals at time multiples of $\pi/2$. As the number of fluctuators is increased the peaks become narrower and smaller, and the $C_Q(\tau,\alpha,N_f)$ is zero almost everywhere. The quantum capacity is thus very sensitive to the channel length or, equivalently,

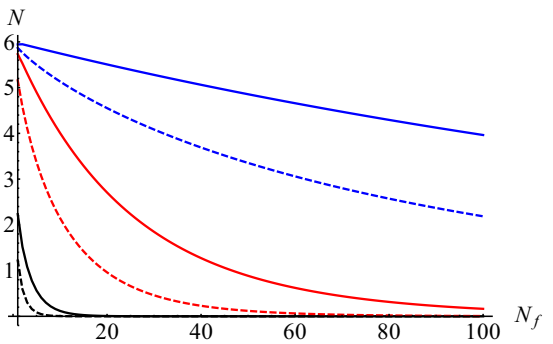


FIG. 4. (Color online) Non-Markovianity of colored channels. The plot shows the non-Markovianity measures as a function of the number of fluctuators. The plot shows $N_{\mathrm{BLP}}$ (solid lines) and $N_{\mathrm{BCM}}$ (dashed lines) as a function of the number of fluctuators for different values of $\alpha$. The three pairs of lines (from top to bottom) refer to $\alpha = 1.0$ (black), $\alpha = 1.5$ (red), and $\alpha = 2$ (blue).

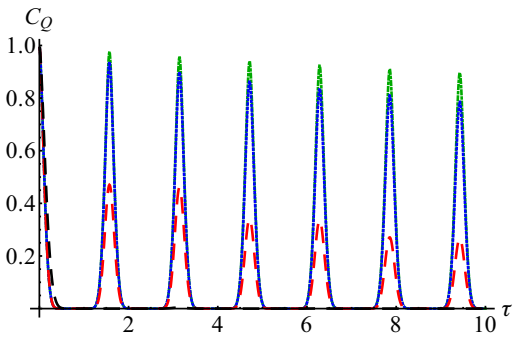


FIG. 5. (Color online) Non-Markovianity of colored channels. The plot shows the quantum capacity for a qubit subject to $1/f^{\alpha}$ noise generated by ten random fluctuators for different values of $\alpha$: $\alpha = 1$ (solid black line), $\alpha = 1.5$ (dashed red line), $\alpha = 2$ (dotted blue line), and $\alpha = 2.5$ (dot-dashed green line).

to the time during which the qubit is subjected to noise. In more detail: only certain lengths of the channel, corresponding to nonzero values of $C_Q(\tau,\alpha,N_f)$, allow for reliable transmission of quantum information. This characteristic lengths depend on the specific parameters of the noise. Besides, the range of nonzero values of $C_Q(\tau,\alpha,N_f)$, decreases as $N_f$ increases, making robust quantum communication a more challenging task. As mentioned above, these conclusions hold upon assuming that the channel is reset after each use, i.e., focusing on memory effects during the propagation and neglecting memory effects among subsequent uses of the channel.

### C. Two-qubits non-Markovianity

We conclude this section by addressing the non-Markovianity of RTN and colored environments acting independently on two dephasing qubits. The dynamics is governed by the Hamiltonian

$$H(t) = H_1(t) \otimes \mathbb{I}_2 + \mathbb{I}_1 \otimes H_2(t), \tag{30}$$

where $H_{1(2)}(t)$ is the single qubit Hamiltonian in Eq. (13) and $\mathbb{I}_{1(2)}$ is the identity operator in the Hilbert space of the first (second) qubit. If we focus on the BLP measure, numerical maximization should be performed to find the maximizing initial pair of states. In both the case of RTN and colored noise, the maximizing pair corresponds to the two orthogonal factorized states $|{+}{+}\rangle$ and $|{-}{-}\rangle$. We have numerically confirmed that the optimal trace distance in this case also takes the form: $D = |\Gamma(t)|$. The BCM non-Markovianity measure is straightforward to calculate as the quantum capacity, it is additive for degradable channels as the one here considered, namely $C_{2q}(\Phi(t)) = 2C_Q(\Phi(t))$, where the subscript $2q$ stands for two qubits. It follows that the non-Markovian dynamics of two qubits subjected to independent RTN or colored noise is simply related to the single-qubit non-Markovianity, and therefore it is quantitatively the same.

## V. CONCLUSIONS

We have addressed open quantum systems made of one or two qubits interacting with a classical random field and evaluated the non-Markovianity of the corresponding noisy maps. In particular, we focused on environments showing non-Gaussian fluctuations, as those described by random telegraph noise and colored noise with spectra of the the form $1/f^{\alpha}$. Upon analyzing the dynamics of both the trace distance and the quantum or entanglement assisted capacity we have shown that the behavior of non-Markovianity based on both measures is qualitatively similar. Besides, we have shown that environments with a spectrum dominated by low-frequency contribution are generally non-Markovian, and that non-Markovianity of colored environments decreases when the number of fluctuators realizing the environment increases.

Overall, our results confirm that non-Markovianity may represent a resource for quantum information processing. In particular, our results show that non-Markovian features are indeed connected to the revivals of quantum correlations. In fact, if we compare our results with those in Ref. [29], we find that whenever the environment is non-Markovian, revivals of quantum correlations are present, while they decay monotonically for a Markovian environment. In other words, our results confirm that non-Markovianity cannot be considered as a mere label to identify different kinds of dynamics. Rather, it may be exploited for a better control of quantum channels, and to better preserve quantum correlations for quantum communication protocols and quantum information processing.

## ACKNOWLEDGMENTS

We acknowledge financial support from the MIUR project FIRB-LiCHIS- RBFR10YQ3H, the Emil Aaltonen Finnish foundation (Non-Markovian quantum information project) and the Scottish Universities Physics Alliance (SUPA). This work was carried out during a visit of C.B., supported by EU through the LLP Erasmus placement program, and M.G.A.P., supported by SUPA visiting professors programme, to Heriot-Watt University. C.B. and M.G.A.P. thank F. Caruso, A. D'Arrigo, P. Bordone, F. Buscemi for useful discussions and Heriot-Watt University for hospitality.

[1] E. Joos, H. D. Zeh, C. Kiefer, D. J. W. Giulini, J. Kupsch, and I.-O. Stamatescu, *Decoherence and the Appearance of a Classical World in Quantum Theory* (Springer, Berlin, 2003).
[2] W. H. Zurek, Rev. Mod. Phys. **75**, 715 (2003).
[3] H.-P. Breuer and F. Petruccione, *The Theory of Open Quantum Systems* (Oxford University Press, Oxford, 2007).
[4] P. Haikka, S. McEndoo, G. De Chiara, G. M. Palma, and S. Maniscalco, Phys. Rev. A **84**, 031602(R) (2011).
[5] S. Lorenzo, F. Plastina, and M. Paternostro, Phys. Rev. A **84**, 032124 (2011).
[6] B.-H. Liu, L. Li, Y.-F. Huang, C.-F. Li, G.-C. Guo, E.-M. Laine, H.-P. Breuer, and J. Piilo, Nature Phys. **7**, 931 (2011).
[7] P. Rebentrost and A. Aspuru-Guzik, J. Chem. Phys. **134**, 101103 (2011).
[8] G. Clos and H.-P. Breuer, Phys. Rev. A **86**, 012115 (2012).

[9] R. Lo Franco, B. Bellomo, S. Maniscalco, and G. Compagno, Int. J. Mod. Phys. B **27**, 1345053 (2013).

[10] S. F. Huelga, A. Rivas, and M. B. Plenio, Phys. Rev. Lett. **108**, 160402 (2012).

[11] A. W. Chin, S. F. Huelga, and M. B. Plenio, Phys. Rev. Lett. **109**, 233601 (2012).

[12] R. Vasile, S. Olivares, M. G. A. Paris, and S. Maniscalco, Phys. Rev. A **83**, 042321 (2011).

[13] E. Laine, H.-P. Breuer, and J. Piilo, arXiv:1210.8266.

[14] B. Bylicka, D. Chruściński, and S. Maniscalco, arXiv:1301.2585v1.

[15] M. M. Wolf, J. Eisert, T. S. Cubitt, and J. I. Cirac, Phys. Rev. Lett. **101**, 150402 (2008).

[16] H.-P. Breuer, E. M. Laine, and J. Piilo, Phys. Rev. Lett. **103**, 210401 (2009).

[17] Á. Rivas, S. F. Huelga, and M. B. Plenio, Phys. Rev. Lett. **105**, 050403 (2010).

[18] X.-M. Lu, X. Wang, and C. P. Sun, Phys. Rev. A **82**, 042103 (2010).

[19] S. Luo, S. Fu, and H. Song, Phys. Rev. A **86**, 044101 (2012).

[20] S. Lorenzo, F. Plastina, and M. Paternostro, Phys. Rev. A **88**, 020102(R) (2013).

[21] M. Mannone, R. Lo Franco and G. Compagno, Phys. Scr. T **153**, 014047 (2013).

[22] R. Lo Franco, B. Bellomo, E. Andersson, and G. Compagno, Phys. Rev. A **85**, 032318 (2012).

[23] J. Helm and W. T. Strunz, Phys. Rev. A **81**, 042314 (2010).

[24] J. Helm, W. T. Strunz, S. Rietzler, and L. E. Würflinger, Phys. Rev. A **83**, 042103 (2011).

[25] Y. M. Galperin, B. L. Altshuler, J. Bergli, and D. V. Shantsev, Phys. Rev. Lett. **96**, 097009 (2006).

[26] L. Faoro and L. Viola, Phys. Rev. Lett. **92**, 117905 (2004).

[27] J. Bergli, Y. M. Galperin, and B. L. Altshuler, Phys. Rev. B **74**, 024509 (2006).

[28] E. Paladino, A. G. Maugeri, M. Sassetti, G. Falci, and U. Weiss, Physica E **40**, 198 (2007).

[29] C. Benedetti, F. Buscemi, P. Bordone, and M. G. A. Paris, Phys. Rev. A **87**, 052328 (2013).

[30] J. Eroms, L. C. van Schaarenburg, E. F. C. Driessen, J. H. Plantenberg, C. M. Huizinga, R. N. Schouten, A. H. Verbruggen, C. J. P. M. Harmans, and J. E. Mooij, Appl. Phys. Lett. **89**, 122516 (2006).

[31] C. E. Parman, N. E. Israeloff, and J. Kakalios, Phys. Rev. B **44**, 8391 (1991).

[32] J. Bergli, Y. M. Galperin, and B. L. Altshuler, New J. Phys. **11**, 025002 (2009).

[33] H. J. Wold, H. Brox, Y. M. Galperin, and J. Bergli, Phys. Rev. B **86**, 205404 (2012).

[34] P. Bordone, F. Buscemi, and C. Benedetti, Fluct. Noise Lett. **11**, 1242003 (2012).

[35] R. Lo Franco, A. D'Arrigo, G. Falci, G. Compagno, and E. Paladino, Phys. Scr. T **147**, 014019 (2012).

[36] M. B. Weissman, Rev. Mod. Phys. **60**, 537 (1988).

[37] A. Ludviksson, R. Kree, and A. Schmid, Phys. Rev. Lett. **52**, 950 (1984).

[38] S. M. Kogan and K. E. Nagaev, Solid State Commun. **49**, 387 (1984).

[39] R. H. Koch, D. P. DiVincenzo, and J. Clarke, Phys. Rev. Lett. **98**, 267003 (2007).

[40] K. Kakuyanagi, T. Meno, S. Saito, H. Nakano, K. Semba, H. Takayanagi, F. Deppe, and A. Shnirman, Phys. Rev. Lett. **98**, 047004 (2007).

[41] E. Paladino, L. Faoro, G. Falci, and R. Fazio, Phys. Rev. Lett. **88**, 228304 (2002).

[42] B. Vacchini, A. Smirne, E.-M. Laine, J. Piilo, and H.-P. Breuer, New J. Phys. **13**, 093004 (2011).

[43] B. Vacchini, J. Phys. B **45**, 154007 (2012).

[44] E-M. Laine, J. Piilo, and H-P. Breuer, Phys. Rev. A **81**, 062115 (2010).

[45] G. M. Palma, K.-A. Suominen, and A. K. Ekert, Proc. R. Soc. London A **452**, 567 (1996).

[46] P. Haikka, T. H. Johnson, and S. Maniscalco, Phys. Rev. A **87**, 010103(R) (2013).

[47] Z. He, J. Zou, L. Li, and B. Shao, Phys. Rev. A **83**, 012108 (2011).

[48] B. Schumacher and M. A. Nielsen, Phys. Rev. A **54**, 2629 (1996).

[49] A. D'Arrigo, G. Benenti, and G. Falci, New J. Phys. **9**, 310 (2007).

[50] M. B. Plenio and S. Virmani, Phys. Rev. Lett. **99**, 120504 (2007); New J. Phys. **10**, 043032 (2008).

[51] F. Caruso, V. Giovannetti, C. Lupo, and S. Mancini, arXiv:1207.5435.

[52] See, e.g., *Special issue on loss of coherence and memory effects in quantum dynamics*, edited by F. Benatti, R. Floreanini, and G. Scholes, J. Phys. B **45**, (2012).

[53] M. Wilde, *Quantum Information Theory* (Cambridge University Press, Cambridge, 2013).

[54] C. Benedetti, F. Buscemi, P. Bordone, and M. G. A. Paris, Int. J. Quantum. Inform. **10**, 1241005 (2012).